**Journal of Magnetics** 17(1), 9-12 (2012) http://dx.doi.org/10.4283/JMAG.2012.17.1.009

# Enhanced Field Emission Behavior from Boron-Doped Double-walled Carbon Nanotubes Synthesized by Catalytic Chemical Vapor Deposition

**J.-H. Kang[1], H. C. Jang[2], J. M. Choi[2], S. C. Lyu[2], and J. H. Sok[2]***

[1]*Department of Nano and Electronic Physics, Kookmin University, Seoul 136-702, Korea*
[2]*Department of Nano Science & Technology, University of Seoul, Seoul 130-743, Korea*

(Received 16 January 2012, Received in final form 19 January 2012, Accepted 26 January 2012)

**Attempts to dope carbon nanotube (CNT) with impurities in order to control the electronic properties of the CNT is a natural course of action. Boron is known to improve both the structural and electronic properties. In this report, we study the field emission properties of Boron-doped double-walled CNT (DWCNT). Boron-doped DWCNT films were fabricated by catalytic decomposition of tetrahydrofuran and triisopropyl borate over a Fe-Mo/MgO catalyst at 900 ºC. We measured the field emission current by varying the doping amount of Boron from 0.8 to 1.8 wt%. As the amount of doped boron in the DWCNT increases, the turn-on-field of the DWCNT decreases drastically from 6 V/μm to 2 V/μm. The current density of undoped CNT is 0.6 mA/cm$^2$ at 9 V, but a doped-DWCNT sample with 1.8 wt% achieved the same current density only at only 3.8 V. This shows that boron doped DWCNTs are potentially useful in low voltage operative field emitting device such as large area flat panel displays.**

**Keywords :** DWCNT, field emission, current density, boron doping

## 1. Introduction

From their early development stages, carbon nanotubes (CNT) have been of interest as potential field emission source materials due to their high aspect ratio and nanometer size diameter. [1] To be a good candidate for a field emitting source materials, it is essential to increase the current density ($J$) to be high enough to achieve low turn-on-fields. Like most semiconductor devices, the electric properties of CNT have been controlled by doping with appropriate impurities. Even for new promising materials such as CNTs and Graphene, the approach to modify their electric properties is the same, i.e. doping with impurities, although CNTs behave as a metal or as a semiconductor depending on its geometric parameters, such as chirality and diameters [2-4]. The choice of doping elements can modify the electronic structure in two major ways: acceptor (B-doping) or donor (N-doping) [5-10]. Efforts to synthesize boron doped CNT are prevalent and use various methodologies including arc discharge [1l], laser vaporization [12], Plasma Enhanced Chemical Vapor Deposition (PECVD) [13] and Catalytic CVD with metallic catalysts [14]. Besides the changed electronic properties, boron doped CNT has shown improved zigzag tube chirality [15], the stiffness [16]. In our previous work, we showed that a catalytic CVD method involving the decomposition of tetrahydrofuran and triisopropyl borate can produce well defined DWCNT with inner and outer diameters in the range of 1.6-2.4 nm. In addition it was demonstrated that the boron concentration in carbon networks can be controllable simply by varying the boron precursor [17].

In this report, we address boron doped DWCNT fabrication and observe their field emission with low turn-on-fields after processing by catalytic CVD.

## 2. Experimental Techniques

The B-doped DWCNT preparation by catalytic chemical vapor deposition (CVD) was carried out in two steps. The first step is making a magnesia (MgO) supported Fe-Mo catalyst. Fe-Mo/MgO was produced by catalytic impregnation, this is the process of making a support material (MgO) containing the desired catalyst (Fe-Mo) with a predetermined weight ratio. The procedure consists embedding a mixed Fe-Mo solution onto porous MgO powder. The mixed Fe-Mo solution consists of

*Corresponding author: Tel: +82-2-2210-5670
Fax: +82-2-2210-5321, e-mail: sokjh@uos.ac.kr

$Fe(NO_3)_3 \cdot 9H_2O$ (Aldrich, 99.99%) and Mo solution (Aldrich, 9.8 mg/ml, Mo in $H_2O$). After evaporating the solvent and grinding into fine powder, a Fe-Mo/MgO catalyst was produced and composed of elements with the desired ratio, Fe:Mo:MgO = 1:0.1:12. The final step for the Fe-Mo/MgO catalyst is calcinations under air ambient at 700 ºC for 7 h.

The second step in the synthesis of B doped DWCNT is carried out by decomposing tettrahydrofuran (THF, $C_4H_8O$, 99.9% Aldrich) and triisopropyl borate ($C_9H_{21}BO_3$, 98%, Aldrich), which are hydrocarbon and boron sources, respectively. Since the THF and triisopropyl borate are in a liquid phase they are contained in a bubbler and fed into reactor with Ar at 1000 sccm. By the process of these gases, $H_2$ (100 sccm) and Ar (1000 sccm with THF and triisopropyl borate), flowing over the Fe-Mo/MgO catalyst in the middle of quartz tube type CVD reactor, the B doped DWCNT is fabricated.

The resultant B-doped DWCNT contains several types of impurity, such as amorphous carbonaceous, MgO support and catalyst metals. To remove these, a purification treatment is performed: the B-doped DWCNT is rinsed by, HCl and $HNO_3$ for 5 h, then DI rinsed and finalized by drying in a vacuum oven for overnight. This purification step is important since the random presence of catalyst residues makes it difficult to obtain uniform field emissions [18].

Before probing field emission characteristics, the fabricated B-doped DWCNT should be deposited in a film. To do this, they were dispersed in sodium dodecyl sulfate (Sigma-aldrich, SDS) and centrifugation was carried out. Then the obtained high purity B-doped DWCNT suspension was sprayed onto an indium tin oxide (ITO) glass plate. The ITO glass was kept at 120 ºC during the spray printing. The microstructures of the printed B-DWCNT were examined by using a transmission electron microscope (TEM) at 200 kV (JEOL-JEM2100F), while the surface morphology was surveyed by field emission scanning electron microscope (Hitachi S-4700, FE-SEM). More details of the experimental procedure for the synthesis are described elsewhere [17, 20, 23].

Field emission measurements were performed in a UHV environment at $5 \times 10^{-7}$ Torr in a diode configuration (cathode-anode) with a separation of 400 μm. A square high voltage pulse was applied between them with a 1/60 duty and 500 Hz and then turn-on-voltage, current density are measured. All field emission measurements were performed at room temperature. Details of the properties of the field emission measurements are available in elsewhere [18].

## 3. Result and Discussions

### 3.1. Structure and morphology

Microanalysis by electron microscope plays an important role in confirming whether the double walled structure is well formed. Fig. 1(a)-(c) shows the TEM image for undoped and B-doped DWCNT (2.1 wt %), showing the presence of double walls. The TEM images revealed that the as-grown CNTs observed in the SEM images consisted mostly of high-quality DWCNT bundles. Fig. 2(a)-(c) are the SEM images of the samples with different boron dopings (0, 2.1, 3.2 wt %). The morphology of all the samples is similar but the density of the filaments decreases as the triisopropyl borate precursor concentration is increased. A highly resolved magnification of the SEM images shows that the CNTs have an average diameters

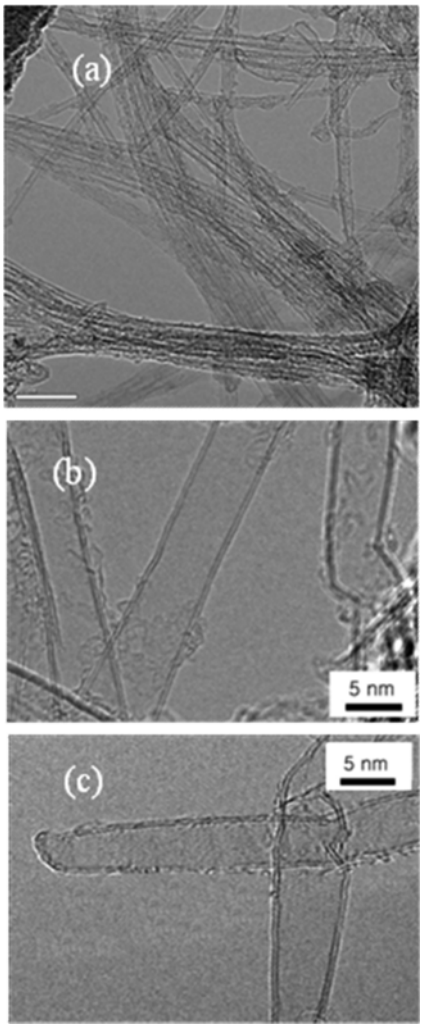


**Fig. 1.** (a) Low magnification TEM image of undoped DWCNT (b) HRTEM image of undoped DWCNT (c) HRTEM image at 2.1 wt %.

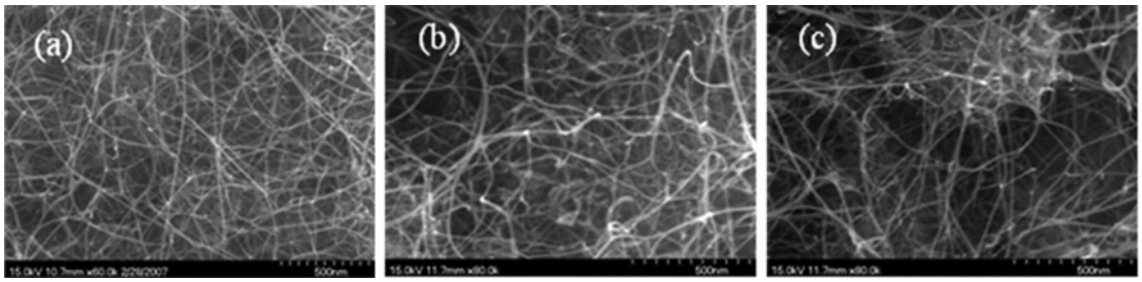


**Fig. 2.** SEM images for (a) 0 wt % (b) 2.1 wt % (c) 3.2 wt %.

of 18-30 nm. It is known that the boron precursor can reduce the activity of the Fe-Mo catalysts surface [17]. Concerning the residue of Fe-Mo catalyst we should note that Fe is a magnetic material and as such can induce magnetism [18, 21, 22] However, according to the TEM analysis the metal catalyst is at undetectable levels so we can say that our purification procedure was very successful in removing catalysts and other impurities.

### 3.2. Field emission properties

Before measuring the field emission properties, tape activation was performed with a view to erecting the CNTs. Fig. 3 shows a tilted SEM image of the samples after the activation and no morphological difference between the doped and undoped DWCNT is evident. Figs. 4 shows current density vs field for the samples, the *J-E* curves are for different boron doping precursor concentrations (0 to 1.8 wt %). For measurement of the 0.8 and 1.8 wt % sample, *J-E* curves were obtained from two different samples ((1) and (2) in Fig. 4) with the same processing conditions to check reproducibility. The curves show that Boron doping is effective for producing CNTs with a low turn-on-field and high current densities. The current density 0.6 mA/cm$^2$ (horizontal arrow in Fig. 4) is reached at only 3.8 V whilst this current density is not reached until 9 V for undoped DWCNTs. The relationship between the field emission current and the electric field is by the following equation [24].

$$I = +A\alpha\Phi^{-1}\frac{\beta^2 V^2}{d^2}\exp\left(-\frac{B\Phi^{3/2}d}{\beta V}\right),$$

where $\alpha$, $\beta$, $\Phi$, $d$ stand for effective area, the field enhancement factor, work function and cathode-anode distance, respectively. A (B) are constants with values of $1.54 \times 10^{-6}$ A·eV·V$^{-2}$ ($6.83 \times 10^{7}$ eV$^{-3/2}$ V·cm$^{-1}$).

The field enhancement factor is a kind of indicator how to external macroscopic field effectively converted and enhanced to microscopic emitter apex. This factor is strongly influenced by geometrical shape such as aspect ratio for a given work function [19].

By X-ray Photoemission Spectroscopy (XPS) analyses in our previous report, it has been confirmed that Boron was successfully substituted into the hexagonal carbon network and the actual doping amount is proportional to the amount of triisopropyl borate precursor concentration

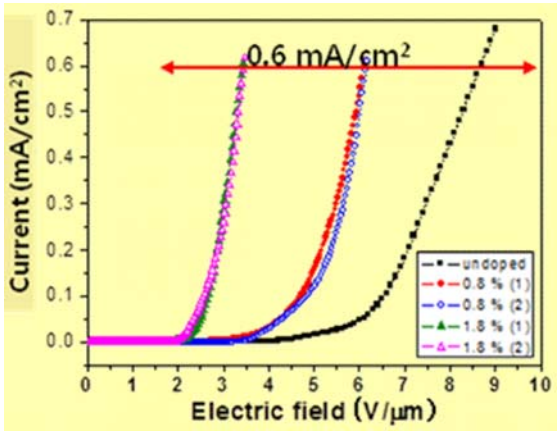


**Fig. 4.** (Color online) *J-E* curves for different doping conditions. (1) and (2) show two different samples that underwent the same processing conditions.

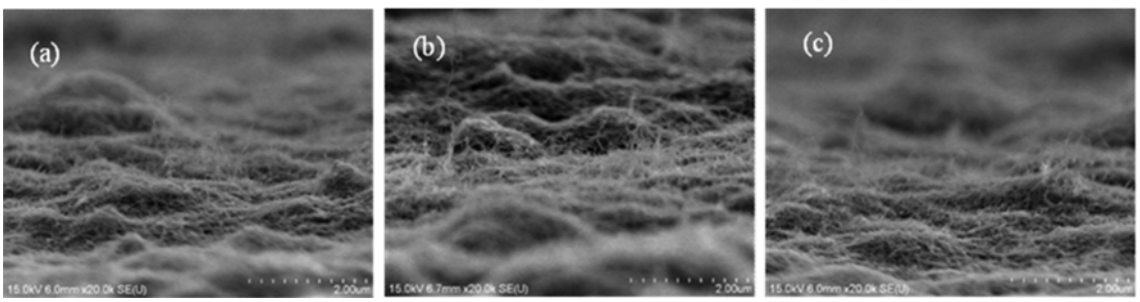


**Fig. 3.** Tilted SEM images of the samples after the activation for (a) undoped (b) 0.8 wt % (c) 1.8 wt %.

used [17]. According to the tight binding and ab initio calculations, the several electronic states of boron saturating the tip edeges of the CNTS are located near to the Fermi level and the reduction of work function by 1.7 eV compared to pure CNT, which are responsible for the high field emission current rather than the field enhancement factor [25]. By simple field emission measurements, however, we cannot determine whether the dominant factor in the enhancement of emission characteristics originates from $\beta$ or the reduction of Φ. According to another paper's theoretical analysis for boron doped SWCNT, the calculated emission current is dependent on both the doping site and the applied field [26]. Compared to results for single wall CNTs this is not surprising since B-doped DWCNT have a more complicated structure, such as the gap between the outer and inner layer. Doped boron can bind to the outer or inner carbon lattice. Boron doping can influence both the electronic structure and the geometric factor, $\beta$.

## 4. Conclusions

We successfully demonstrated the synthesis of B-doped DWCNTs using catalytic CVD by decomposing tetrahydrofuran and triisopropyl borate. This study makes the first observations of field emission from B-doped DWCNT processed by this methodology. Our findings include enhanced current density reached at low fields (e.g. ca. 0.6 mA/cm$^2$ at 3.8 V) and a low turn-on-field (e.g. ca. 2 V/μm).

## Acknowledgement

This work was supported by National Research Foundation of Korea (Grant No. 2011-0012851) and this work was also supported by research program 2009 of Kookmin University in Korea. (J.-H. Kang)

## References

[1] W. A. Heer, A. Chatelain, and D. Ugarte, Science **270**, 5379 (1995).
[2] X. Wang, X. Li, L. Zhaning, Y. Yoon, P. K. Weber, H. Wang, J. Guo, and H. Dai, Science **324**, 5928 (2009).
[3] R. Saito, M. Fujia, G. Dresselhaus, and M. S. Dresselhaus, Appl. Phys. Lett. **60**, 220419 (1992).
[4] N. Hamada, S. Sawda, and A. Oshiyama, Appl. Phys. Lett. **68**, 1579 (1992).
[5] M. Endo, T. Hayashi, S. H. Hong, T. Enoki, and M. S. Dresselhaus, J. Appl. Phys. **90**, 5670 (2001).
[6] L. R. Radovic, M. Karra, K. Skokova, and P. A. Thrower, Carbon **36**, 1841 (1998).
[7] K. Liu, P. Avouris, R. Martel, and W. K. Hsu, Phys. Rev. B. **63**, 1611404 (2001).
[8] K. Y. Chun, H. S. Lee, and C. J. Lee, Carbon **47**, 169 (2009).
[9] C. J. Lee, S. C. Lyu, H. W. Kim, J. H. Lee, and K. I. Cho, Chem. Phys. Lett. **359**, 115 (2002).
[10] J. W. Jang, C. E. Lee, S. C. Lyu, and T. J. Lee, Appl. Phys. Lett. **84**(15), 2877 (2004).
[11] Ph. Redlich, J. Loeffler, P. M. Ajayan, J. Bill, F. Aldinger, and M. Rühle, Chem. Phys. Lett. **260**, 465 (1996).
[12] K. McGuire, N. Gohard, P. L. Gai, M. S. Dresselhaus, G. Sumanasekera, and A. M. Rao, Carbon **43**, 219 (2005).
[13] C. F. Chen. C. L. Tsai, and C. L. Lin, Diam. Relat. Mater. **12**, 1500 (2003).
[14] Paola Ayala, W. Plank, A. Gruneis, E. I. Kauppinen, M. H. Rummeli, H. Kuzmany, and T. Pichler, J. Mater. Chem. **18**, 5676 (2008).
[15] X. Blasé, J.-C. Charlier, A. D. Vita, and R. Car, Phys. Rev. Lett. **83**, 5078 (1999).
[16] A. Agarwal, H. Yinnon, D. R. Uhlmann, R. T. Pepper, and C. R. Desper, J. Mater. Sci. **21**, 3455 (1986).
[17] S. C. Lyu, J. H. Han, K. W. Shin, and J. H. Sok, Carbon **49**, 1532 (2011).
[18] R. B. Rakhi, X. Lim, X. Gao, Y, Yang, A. T. S. Wee, K. Sethupathi, S. Ramaprabhu, and C. H. Sow, Appl. Phys. A **98**, 195 (2010).
[19] E. S. Jang, J. C. Goak, H. S. Lee, J. H. Han, C. S. Lee, J. H. Sok, Y. H. Seo, K. S. Park, and N. S. Lee, Appl. Surf. Sci. **256**, 6838 (2010).
[20] SeungChul Lyu, Dami Jung, KiTae Ahn, Hansung Lee, Naesung Lee, Yunsun Park, and Junghyun Sok, Kor. J. Met. Mater. **48**, 355 (2009).
[21] B. Bittova, J. Poltiverova Vejpravova, M. Kalbac, S. Burianova, A. Mantlikova, S. Danis, and S. Doyle, J. Phys. Chem. C **115**, 17303 (2011).
[22] Yuji Fujiwara, Hitoshi Takegawa, Hideki Sato, Kohji Maeda, Yahachi Saito, Tadashi Kobayashi, and Shigeru Shiomi. J. Appl. Phys. **95**, 7119 (2004).
[23] KiTae Ahn, HyunChul Jang, SeungChul Lyu, Hansung Lee, Naesung Lee, Moonsup Han, Yunsun Park, Wanshick Hong, Kyoungwan Park, and Junghyun Sok, Kor. J. Met. Mater. **49**, 79 (2010).
[24] R. H. Fowler and L. Nordheim, Proc. R. Soc. London Ser. A. **119**, 173 (2005).
[25] J.-C. Charlier, M. Terrones, M. Baxendale, V. Meunier, T. Zacharia, N. L. Rupensinghe, W. K. Hsu, N. Gerbert, H. Terrones, and G. A. J. Amaratunga, Nano Letters **2**, 1191 (2002).
[26] Hyo-Shin Ahn, Kwang-Ryeol Lee, Doh-Yeon Kim, and Sengwu Han, Appl. Phys. Lett. **88**, 093122 (2006).